SCIENCE CHINA
Information Sciences

• RESEARCH PAPER •

Leader-follower formation of vehicles with velocity constraints and local coordinate frames

Xiao YU & Lu LIU*

Department of Mechanical and Biomedical Engineering, City University of Hong Kong, Kowloon, Hong Kong SAR, China.

Abstract This paper studies leader-follower formation control of networked nonholonomic vehicles of unicycle type. Each vehicle is subject to the velocity constraints consisting of saturated angular velocity and bounded linear velocity with positive-minimum value. Each vehicle is allowed to use its local coordinate frame, and the network topology is described by a directed graph containing a spanning tree. Two dynamic control laws satisfying the velocity constraints are developed respectively, such that the leader-follower formation defined in local coordinate frames can be achieved in two cases. The proposed control laws only require each vehicle to use the information of its neighbors in the network via local measurements and communication. Finally, effectiveness is illustrated by simulation results of an example.

Keywords Formation control, local coordinate frame, mobile robot, nonholonomic vehicle, velocity constraint

Citation Yu X, Liu L. Leader-follower formation of vehicles with velocity constraints and local coordinate frames. Sci China Inf Sci, 2016, 59(1): xxxxxx, doi: xxxxxxxxxxxxxx

1 Introduction

Distributed multi-agent coordination has been an active topic since the last decade [1, 12]. Due to the rapid development of technology on unmanned vehicles, such as autonomous underwater vehicles (AUVs), unmanned aerial vehicles (UAVs), mobile wheeled robots (MWRs), tethered space robots (TSRs) [5], formation control of multi-vehicle systems has attracted much research interest, see [2, 8, 11, 17, 19] and the reference therein. In particular, many works focus on vehicles of unicycle type [6], since unicycle can be used to describe the simplified model of a UAV and an MWR [13]. In practice, the linear velocity and angular velocity of a vehicle is bounded due to the thrust limitations. Besides, many vehicles are subject to the stall condition such that they need to maintain a positive-minimum linear velocity, e.g., a fixed-wing UAV [14]. Thus, it is of practical meaning to take into account these velocity constraints in formation control of vehicles.

One fundamental formation control problem is to make each follower vehicle maintain a desired relative position to the leader and follow the leader's motion. Several works studied this leader-follower formation control problem of vehicles subject to the velocity constraints. This problem reduces to trajectory tracking control problem when only one follower is considered and the desired relative position equals zero. To

* Corresponding author (email: luliu45@cityu.edu.hk)

address the velocity constraints, the authors in [14] developed a controller by using constrained control Lyapunov functions. In [4], an additive uncertainty in vehicle dynamics was considered. Some works studied multiple vehicles and considered the case where the desired relative position to the leader is defined in inertial frame. In [9] and [10], the authors studied vehicles under static and time-varying relative position sensor digraphs respectively. It was shown that the constraint of positive-minimum linear velocity can be satisfied and broadcast communication was required for the leader to send its information to all followers. In [18], the proposed control law only required each vehicle to use local information and information from its neighbors, and all aforementioned velocity constraints can be satisfied. However, an inertial frame implies a common reference direction for all vehicles. For vehicles with only local coordinate frames, the authors in [3] and [15] studied the case with only one follower vehicle. It was shown in [3] that the follower can stay in an arc of the circle centered in the leader's frame while the leader moves. In [15], the follower vehicle was made to converge to a desired relative position defined in the leader's frame when the linear velocity of leader is an unknown constant. In [7], the authors studied multiple vehicles under a network of which the topology is modeled by a directed acyclic graph. It was shown that the formation tracking errors can only converge to a neighborhood of zero.

In this paper, we propose a distributed dynamic control law for unicycle-type vehicles with velocity constraints and local coordinate frames, such that the leader-follower formation can be achieved in two cases. Each follower only uses the information of its neighbors in a network by local measurements and communication. The network topology is described by a directed graph containing a spanning tree. The velocity constraints including the constraint of positive-minimum linear velocity are taken into account. Different from [9, 10, 18], the desired leader-follower formation is described by relative positions defined in leader's coordinate frame.

The main contributions of this work can be summarized into three aspects. First, the proposed control law allows vehicles with velocity constraints to use local coordinate frames, such that leader-follower formation can be achieved in two cases. Compared with [9, 10, 18], vehicles are not required to share a common reference direction. Second, compared with [7], the network topology is not limited to a directed acyclic graph and the formation tracking errors can converge to zero in two cases. Third, compared with [15], multiple followers instead of only one follower are considered, and the linear velocity of leader is allowed to be time-varying. Besides, the relative heading angles with respect to the leader can converge to zero.

The rest of this paper is organized as follows. Section 2 presents the problem formulation and a technical lemma. In Section 3, distributed formation control laws are proposed and stability analysis of the closed-loop systems is presented. Section 4 shows simulation results of illustrative examples, which is followed by the conclusions in Section 5.

2 Preliminaries

2.1 Problem Formulation

Consider a group of $N+1$ nonholonomic vehicles of unicycle type. The kinematic model of vehicle i is described by:

$$\dot{x}_i = v_i \cos\theta_i,\ \ \dot{y}_i = v_i \sin\theta_i,\ \ \dot{\theta}_i = \omega_i,\ \ i = 0, 1, ..., N, \tag{1}$$

where $\boldsymbol{p}_i := [x_i\ y_i]^{\mathrm{T}} \in \mathbb{R}^2$ is the absolute position and $\theta_i \in \mathbb{R}$ is the heading angle in the inertial frame. $v_i \in \mathbb{R}$ and $\omega_i \in \mathbb{R}$ are the linear velocity and angular velocity respectively, which are regarded as the control inputs. Note that θ_i and $\theta_i + 2K_i\pi$ with $K_i \in \mathbb{Z}$ represent the same orientation in practice.

The following physical velocity constraints [14] of each vehicle are considered:

$$v_i \in [v_{\min},\ v_{\max}], \qquad v_{\max} > v_{\min} > 0, \tag{2}$$

$$\omega_i \in [-\omega_{\max},\ \omega_{\max}],\ \omega_{\max} > 0. \tag{3}$$

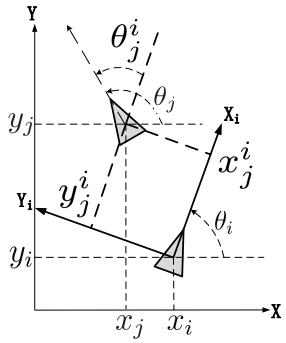

Fig. 1 Illustration of the local coordinate frame.

The group of vehicles contains one uncontrolled vehicle labeled 0, and it is called leader. The others labeled i, $i = 1, ..., N$, are followers. The leader which decides the group motion satisfies the following assumption:

Assumption 1. $v_0(t)$ and $\omega_0(t)$ are bounded, i.e., $v_0(t) \in [\underline{v},\ \overline{v}]$, $\omega_0(t) \in [-\overline{\omega},\ \overline{\omega}]$, $\forall t \geqslant t_0$, where $\underline{v}$, $\overline{v}$, and $\overline{\omega}$ are known constants satisfying $[\underline{v},\ \overline{v}] \subseteq [v_{\min},\ v_{\max}]$ and $[-\overline{\omega},\ \overline{\omega}] \subseteq [-\omega_{\max},\ \omega_{\max}]$. ■

In practice, the acceleration of a vehicle is bounded and thus the following assumption is made:

Assumption 2. $\dot{v}_0(t)$ exists and is bounded for all $t \geqslant t_0$. ■

Each vehicle only has access to the information of its neighbors in a network. The network topology is modeled by a directed graph $\bar{\mathcal{G}}$ described as follows. First, a directed graph $\mathcal{G} = \{\mathcal{O}, \mathcal{E}\}$ is used to model the network among N followers. The directed graph $\mathcal{G}$ consists of a finite set of nodes $\mathcal{O} = \{1, ..., N\}$ representing N follower vehicles, and a set of edges $\mathcal{E} \subseteq \{(j, i) : j \neq i, i, j \in \mathcal{O}\}$, containing directed edges from node j to node i. Then, combining $\mathcal{G}$ and node 0 (leader) yields the directed graph $\bar{\mathcal{G}} = \{\bar{\mathcal{O}}, \bar{\mathcal{E}}\}$, where $\bar{\mathcal{O}} = \mathcal{O} \cup \{0\}$, and $\bar{\mathcal{E}} = \mathcal{E} \cup \{(0, i)\},\ i \in \mathcal{O}$. A directed edge $(j, i),\ j, i \in \bar{\mathcal{O}}$, means that the information of vehicle j is available to vehicle i. Node j is a neighbor of node i if $(j, i) \in \mathcal{E}$, and a set $\mathcal{N}_i \subseteq \mathcal{O}$ denotes all neighbors of node i. Define $a_{ij} = 1$ if $(j, i) \in \bar{\mathcal{E}}$, otherwise $a_{ij} = 0$, and denote the Laplacian matrix of $\bar{\mathcal{G}}$ by $\bar{\mathcal{L}}$. The following assumption is made on the directed graph $\bar{\mathcal{G}}$:

Assumption 3. The directed graph $\bar{\mathcal{G}}$ contains a directed spanning tree with node 0 being the root. ■

The network among vehicles is physically set up by the onboard sensor and communication device of each vehicle. Different from [9,10,18], we assume that vehicles do not have a common reference direction. Thus, the relative position $\boldsymbol{p}_i - \boldsymbol{p}_j$, $j \in \bar{\mathcal{N}}_i$, and the heading angle θ_i cannot be measured. In this case, each vehicle uses its local coordinate frame, i.e., the Frenet-Serret frame, see Fig. 1 for illustration. Then, $\boldsymbol{p}_j$ and θ_j measured in the coordinate frame of vehicle i can be expressed as

$$\boldsymbol{p}_j^i := [x_j^i\ y_j^i]^{\mathrm{T}} = R(\theta_i)(\boldsymbol{p}_j - \boldsymbol{p}_i),\ \theta_j^i = \theta_j - \theta_i, \tag{4}$$

respectively, where $R(\cdot) = \begin{bmatrix} \cos(\cdot) & \sin(\cdot) \\ -\sin(\cdot) & \cos(\cdot) \end{bmatrix}$.

The leader-follower formation considered in this paper is defined in the local coordinate frames. The objective is to design a controller for vehicle i, $i = 1, ..., N$, such that $\boldsymbol{p}_0^i$ converges to $\boldsymbol{p}_0^i + \boldsymbol{h}_{0i}$ and $\theta_0^i(t)$ converges to $2K_i\pi$ with $K_i \in \mathcal{Z}$, where the constant vector $\boldsymbol{h}_{0i}$ denotes the desired relative position to the leader in the local coordinate frame of vehicle i. By default, $\boldsymbol{h}_{00} = \boldsymbol{0}$. Note that $\theta_0^i = 0$ and $\theta_0^i = 2K_i\pi$ represent the same orientation, and θ_j^i is generally measured in $(-2\pi, 2\pi)$ in practice.

Now, the *leader-follower formation control problem* considered in this paper is formally stated as follows:

Problem 1. Consider N follower vehicles and a leader vehicle. Given a directed graph $\bar{\mathcal{G}}$, for all initial states $\boldsymbol{p}_0^i(t_0) \in \mathbb{R}^2$ and $\theta_0^i(t_0) \in (-2\pi, 2\pi)$, $i = 1, ..., N$, $\forall t_0 \geqslant 0$, find a dynamic control law in the form of

$$[\omega_i\ v_i]^{\mathrm{T}} = \boldsymbol{\varrho}(\boldsymbol{\rho}_0^i, \boldsymbol{p}_j^i, \theta_j^i),\ \dot{\boldsymbol{\rho}}_0^i = \boldsymbol{\kappa}(\boldsymbol{\rho}_0^i, \boldsymbol{\rho}_0^j, \boldsymbol{p}_j^i, \theta_j^i), j \in \bar{\mathcal{N}}_i, \tag{5}$$

such that

$$\lim_{t\to\infty} \boldsymbol{p}_0^i(t) + \boldsymbol{h}_{0i} = 0, \ \lim_{t\to\infty} \theta_0^i(t) = 0, \ i = 1, ..., N, \tag{6}$$

where $\boldsymbol{\rho}_0^i$, to be designed later, is an estimate of the information associated with the leader, functions $\boldsymbol{\varrho}(\cdot)$ and $\boldsymbol{\kappa}(\cdot)$ are sufficiently smooth, and $\boldsymbol{\varrho}(\cdot)$ is properly bounded. ■

2.2 Technical Lemmas

The following lemma can be referred to as a comparison principle for vectorial differential equations. Say that $\boldsymbol{x} \leqslant \boldsymbol{y}$ for $\boldsymbol{x}, \ \boldsymbol{y} \in \mathbb{R}^n$ if the entries of $\boldsymbol{x}$ and $\boldsymbol{y}$ satisfy $x_i \leqslant y_i$, $i = 1, ..., n$.

Lemma 1. Consider the vectorial differential equation $\dot{\boldsymbol{y}} = \boldsymbol{f}(t, \boldsymbol{y})$ with $\boldsymbol{y} = [y_1, ..., y_n]^{\mathrm{T}} \in \mathbb{R}^n$ and $\boldsymbol{f}(t, \boldsymbol{y}) = [f_1(t, \boldsymbol{y}), \cdots, f_n(t, \boldsymbol{y})]^{\mathrm{T}}$, where $f_i(t, \boldsymbol{y})$ is differentiable in t and locally Lipschitz in $\boldsymbol{y}$, for all $t \geqslant t_0$ and all $\boldsymbol{y} \in \Psi$ with Ψ being any subset of $\mathbb{R}^n$. Let $[t_0, T)$ (T could be infinity) be the maximal interval of existence of the solution $\boldsymbol{y}(t)$ and suppose $\boldsymbol{y}(t) \in \Psi$ for all $t \in [t_0, T)$. Let $\boldsymbol{x}(t) \in \mathbb{R}^n$ be a continuous function of which the upper right-hand derivative $D^+\boldsymbol{x}(t)$ satisfy the differential inequality

$$D^+\boldsymbol{x}(t) \leqslant \boldsymbol{f}(t, \boldsymbol{x}(t)), \ \boldsymbol{x}(t_0) \leqslant \boldsymbol{y}(t_0), \tag{7}$$

with $\boldsymbol{x}(t) \in \Psi$ for all $t \in [t_0, T)$. If for any $i \neq j$,

$$\frac{\partial f_i(t, \boldsymbol{x})}{\partial x_j} \geqslant 0, \tag{8}$$

then $\boldsymbol{x}(t) \leqslant \boldsymbol{y}(t)$ for all $t \in [t_0, T)$. ■

The proof is given in Appendix A.

3 Main Results

In this section, we solve Problem 1 in two cases. For each case, a distributed dynamic control law is proposed. In the first case, the leader vehicle is assumed to move in a linear motion. In the second case, this assumption is removed but the desired relative position $\boldsymbol{h}_{0i}$ is limited.

3.1 Case 1: A Leader Moving in a Linear Motion

In this case, we assume that the leader is moving in a linear motion. As in [18], the desired relative position $\boldsymbol{h}_{0i}$ is not known to vehicle i, and each follower vehicle i only knows a constant vector $\boldsymbol{h}_{ji}$, $j \in \bar{\mathcal{N}}_i$, which denotes the desired relative position to vehicle j in the local coordinate frame of vehicle i. The assumption on Case 1 is summarized as follows.

Assumption 4. The angular velocity of the leader satisfies $\omega_0(t) = 0$, $\forall t \geqslant t_0$. Each follower vehicle i does not know $\boldsymbol{h}_{0i}$ and only knows $\boldsymbol{h}_{ji}$, $j \in \bar{\mathcal{N}}_i$. ■

First, define the tracking error $\boldsymbol{p}_{ei} = [x_{ei} \ y_{ei}]^{\mathrm{T}}$ as

$$\boldsymbol{p}_{ei} = \boldsymbol{p}_0^i + R(-\theta_0^i)\boldsymbol{h}_{0i}, \ \theta_{ei} = \theta_0^i. \tag{9}$$

Taking its time derivative yields the following error dynamics:

$$\dot{\boldsymbol{p}}_{ei} = \omega_i S \boldsymbol{p}_{ei} + v_0 \begin{bmatrix} \cos\theta_{ei} \\ \sin\theta_{ei} \end{bmatrix} - v_i Q, \ \dot{\theta}_{ei} = -\omega_i, \tag{10}$$

where $S = \begin{bmatrix} 0 & 1 \\ -1 & 0 \end{bmatrix}$ and $Q = \begin{bmatrix} 1 \\ 0 \end{bmatrix}$.

To solve Problem 1, it suffices to show that $\boldsymbol{p}_e = \mathrm{col}(\boldsymbol{p}_{e1}, ..., \boldsymbol{p}_{eN})$ and $\boldsymbol{\theta}_e = \mathrm{col}(\theta_{e1}, ..., \theta_{eN})$ converge to zero as $t \to \infty$.

However, $\boldsymbol{p}_{ei}$, θ_0^i, and v_0 are not known to the follower vehicles. In this case, set an internal state $[\hat{\boldsymbol{p}}_{ei}^{\mathrm{T}}\ \hat{\theta}_{ei}\ \hat{v}_i]^{\mathrm{T}}$ for each vehicle i. Let $\hat{\boldsymbol{p}}_{ei}$, $\hat{\theta}_{ei}$, and $\hat{v}_i$ be the estimate of $\boldsymbol{p}_{ei}$, θ_{ei}, and v_0 for vehicle i respectively.

Then, we propose a dynamic control law for each follower vehicle i as follows.

$$v_i = \mathrm{sat}(\hat{v}_i, \overline{v}, \underline{v}) + \frac{k_1 \hat{x}_{ei}}{\sqrt{1+\hat{\boldsymbol{p}}_{ei}^{\mathrm{T}}\hat{\boldsymbol{p}}_{ei}}}, \tag{11}$$

$$\omega_i = \frac{k_3 \sin\frac{\hat{\theta}_{ei}}{2}}{\sqrt{1+\hat{\boldsymbol{p}}_{ei}^{\mathrm{T}}\hat{\boldsymbol{p}}_{ei}}} + \frac{k_2\,\mathrm{sat}(\hat{v}_i, \overline{v}, \underline{v})(\hat{y}_{ei}\cos\frac{\hat{\theta}_{ei}}{2} - \hat{x}_{ei}\sin\frac{\hat{\theta}_{ei}}{2})}{\sqrt{1+\hat{\boldsymbol{p}}_{ei}^{\mathrm{T}}\hat{\boldsymbol{p}}_{ei}}}, \tag{12}$$

$$\dot{\hat{\boldsymbol{p}}}_{ei} = \omega_i S\hat{\boldsymbol{p}}_{ei} + \hat{v}_i[\cos\hat{\theta}_{ei}\ \ \sin\hat{\theta}_{ei}]^{\mathrm{T}} - v_i Q + \mu\sum_{j\in\bar{\mathcal{N}}_i} a_{ij}(R(-\theta_j^i)\hat{\boldsymbol{p}}_{ej} - \hat{\boldsymbol{p}}_{ei} + \boldsymbol{p}_j^i + R(-\hat{\theta}_{ei})\boldsymbol{h}_{ji}), \tag{13}$$

$$\dot{\hat{\theta}}_{ei} = -\omega_i + \mu\sum_{j\in\bar{\mathcal{N}}_i} a_{ij}(\hat{\theta}_{ej} - \hat{\theta}_{ei} + \theta_j^i), \tag{14}$$

$$\dot{\hat{v}}_i = \frac{1}{\sum\limits_{j\in\mathcal{N}_i} a_{ij}} \sum_{j\in\bar{\mathcal{N}}_i} a_{ij}(\dot{\hat{v}}_j + \mu(\hat{v}_j - \hat{v}_i)), \tag{15}$$

where μ is any positive constant, $k_1,\ k_2$, and k_3 are positive constants satisfying

$$k_1 \leqslant \min(v_{\max} - \overline{v},\ \underline{v} - v_{\min}),\ 2k_2\overline{v} + k_3 \leqslant \omega_{\max}. \tag{16}$$

Function $z = \mathrm{sat}(a, b, c) : \mathbb{R}^3 \mapsto \mathbb{R}$ is defined as $z = a$, if $c \leqslant a \leqslant b$; $z = b$, if $a > b$ and $z = c$, if $a < c$. The initial state $[\hat{\boldsymbol{p}}_{ei}^{\mathrm{T}}(t_0)\ \hat{\theta}_{ei}(t_0)\ \hat{v}_i(t_0)]^{\mathrm{T}}$ can be arbitrarily selected in $\mathbb{R}^2\times\mathbb{R}\times\mathbb{R}$. By default, $\hat{\boldsymbol{p}}_{e0} = [0\ 0]^{\mathrm{T}}$ and $[\hat{\theta}_{e0}\ \hat{v}_0]^{\mathrm{T}} = [0\ v_0]^{\mathrm{T}}$.

To implement dynamic control law (11)–(15), the onboard sensors of vehicle i is required to measure the relative states $\boldsymbol{p}_j^i$ and θ_j^i in its local coordinate frame, and the communication device of vehicle i is used to receive the information $[\hat{\boldsymbol{p}}_{ej}^{\mathrm{T}}\ \hat{\theta}_{ei}\ \hat{v}_i]^{\mathrm{T}}$ from its neighbors. The design of (13)–(15) are based on the information of vehicle i and the information from its neighbors, and thus can be viewed as a distributed observer. Then, dynamic control law (11)–(15) can be described in the form of (5).

Before the main result of Case 1 is presented, a property of the distributed observer (13)–(15) is given in the following proposition. This property is required in establishing the stability analysis for the main result of Case 1.

Proposition 1. Consider the distributed observer (13)–(15), a leader vehicle and directed graph $\bar{\mathcal{G}}$. Under Assumptions 1–4, for any initial states $[\hat{\boldsymbol{p}}_{ei}^{\mathrm{T}}(t_0)\ \hat{\theta}_{ei}(t_0)\ \hat{v}_i(t_0)]^{\mathrm{T}}$, $i = 1, ..., N$, $\forall t_0 \geqslant 0$, each $[\hat{\boldsymbol{p}}_{ei}^{\mathrm{T}}(t)\ \hat{\theta}_{ei}(t)\ \hat{v}_i(t)]^{\mathrm{T}}$ converges to $[\boldsymbol{p}_{ei}^{\mathrm{T}}(t_0)\ \theta_0^i(t)\ v_0(t)]^{\mathrm{T}}$ *exponentially* as $t\to\infty$. ∎

Proof. Define

$$\tilde{\boldsymbol{p}}_{ei} := [\tilde{x}_{ei}\ \tilde{y}_{ei}] = \hat{\boldsymbol{p}}_{ei} - \boldsymbol{p}_{ei},\ \tilde{\theta}_{ei} = \hat{\theta}_{ei} - \theta_{ei},\ \tilde{v}_i = \hat{v}_i - v_0. \tag{17}$$

Note that the Laplacian matrix $\bar{\mathcal{L}}$ of the digraph $\bar{\mathcal{G}}$ can be partitioned as follows:

$$\bar{\mathcal{L}} = \left(\begin{array}{c|c} 0 & 0 \\ \hline -\mathcal{A}_0\mathbf{1}_N & H \end{array}\right), \tag{18}$$

where $\mathcal{A}_0 = \mathrm{diag}(a_{10}, ..., a_{N0})$. By Assumption 3 and Lemma 1 in [16], H is nonsingular and all eigenvalues of H have positive real parts. Then, $-H$ is Hurwitz and there exist $\alpha_1,\ \beta_1 > 0$ such that

$$\|e^{-\mu H s}\| \leqslant \alpha_1 e^{-\beta_1 s},\ \forall s \geqslant 0. \tag{19}$$

Using (14) and (17) gives

$$\dot{\tilde{\theta}}_{ei} = \mu\sum_{j\in\bar{\mathcal{N}}_i} a_{ij}(\tilde{\theta}_{ej} - \tilde{\theta}_{ei}). \tag{20}$$

Denoting $\tilde{\boldsymbol{\theta}}_e = \mathrm{col}(\tilde{\theta}_{e1}, ..., \tilde{\theta}_{eN})$, N systems in the form of (20) can be rewritten into the following compact form:

$$\dot{\tilde{\boldsymbol{\theta}}}_e = -\mu H \tilde{\boldsymbol{\theta}}_e. \tag{21}$$

Thus, $\tilde{\boldsymbol{\theta}}_e(t) = e^{-\mu H(t-t_0)}\tilde{\boldsymbol{\theta}}_e(t_0)$ and it follows from (19) that $\tilde{\boldsymbol{\theta}}_e(t)$ converges to zero as $t \to \infty$.

Using (15) and (17) yields

$$\sum_{j\in\mathcal{N}_i} a_{ij}(\dot{\tilde{v}}_j - \dot{\tilde{v}}_i) = -\mu \sum_{j\in\mathcal{N}_i} a_{ij}(\tilde{v}_j - \tilde{v}_i). \tag{22}$$

Defining $\delta_i = \sum_{j\in\bar{\mathcal{N}}_i} a_{ij}(\tilde{v}_j - \tilde{v}_i)$, (22) becomes

$$\dot{\delta}_i = -\mu\delta_i,\ i = 1, ..., N. \tag{23}$$

Then, denote $\tilde{\boldsymbol{v}} = \mathrm{col}(\tilde{v}_1, ..., \tilde{v}_N)$, and we can obtain

$$[\delta_1, ..., \delta_N]^{\mathrm{T}} = \mu H \tilde{\boldsymbol{v}}. \tag{24}$$

It follows from (23) that $\delta_i(t) = e^{-(t-t_0)}\delta_i(t_0)$. Thus, $\tilde{\boldsymbol{v}}$ converges to zero exponentially as $t \to \infty$.

Next, it follows from

$$R(-\theta_j^i)\boldsymbol{p}_{ej} + \boldsymbol{p}_j^i + R(-\hat{\theta}_{ei})\boldsymbol{h}_{ji} = \boldsymbol{p}_{ei}, \tag{25}$$

(10), (13), and (17) that

$$\dot{\tilde{\boldsymbol{p}}}_{ei} = \omega_i S\tilde{\boldsymbol{p}}_{ei} + \mu \sum_{j\in\bar{\mathcal{N}}_i} a_{ij}(R(-\theta_j^i)\tilde{\boldsymbol{p}}_{ej} - \tilde{\boldsymbol{p}}_{ei}) + \boldsymbol{\Delta}_i, \tag{26}$$

where $\boldsymbol{\Delta}_i$ is defined as

$$\boldsymbol{\Delta}_i = (\hat{v}_i - v_i)\begin{bmatrix}\cos\hat{\theta}_{ei}\\ \sin\hat{\theta}_{ei}\end{bmatrix} + v_i\begin{bmatrix}\cos\hat{\theta}_{ei} - \cos\theta_{ei}\\ \sin\hat{\theta}_{ei} - \sin\theta_{ei}\end{bmatrix}. \tag{27}$$

Consider a Lyapunov function candidate

$$V(\tilde{\boldsymbol{p}}_{ei}) = \frac{1}{2}\tilde{\boldsymbol{p}}_{ei}^{\mathrm{T}}\tilde{\boldsymbol{p}}_{ei},$$

and taking its time derivative along the trajectories of (26) leads to

$$\begin{aligned}\dot{V}(\tilde{\boldsymbol{p}}_{ei}) &= \frac{1}{2}\omega_i(S + S^{\mathrm{T}})\tilde{\boldsymbol{p}}_{ei} + \frac{1}{2}(\tilde{\boldsymbol{p}}_{ei}^{\mathrm{T}}\boldsymbol{\Delta}_i + \boldsymbol{\Delta}_i^{\mathrm{T}}\tilde{\boldsymbol{p}}_{ei}) + \mu\sum_{j\in\bar{\mathcal{N}}_i} a_{ij}(\frac{1}{2}(\tilde{\boldsymbol{p}}_{ei}^{\mathrm{T}}R(\theta_i^j)\tilde{\boldsymbol{p}}_{ej} + \tilde{\boldsymbol{p}}_{ej}^{\mathrm{T}}R(\theta_i^j)\tilde{\boldsymbol{p}}_{ei}) - \tilde{\boldsymbol{p}}_{ei}^{\mathrm{T}}\tilde{\boldsymbol{p}}_{ei})\\ &\leqslant \|\boldsymbol{\Delta}_i\|\|\tilde{\boldsymbol{p}}_0^i\| + \mu\sum_{j\in\bar{\mathcal{N}}_i} a_{ij}(\|\tilde{\boldsymbol{p}}_{ej}\|\|\tilde{\boldsymbol{p}}_{ei}\| - \|\tilde{\boldsymbol{p}}_{ei}\|^2).\end{aligned} \tag{28}$$

Define $\bar{\boldsymbol{p}}_{ei} = \|\tilde{\boldsymbol{p}}_{ei}\|$. Since $V(\tilde{\boldsymbol{p}}_{ei}) = V(\bar{\boldsymbol{p}}_{ei}) = \frac{1}{2}\bar{\boldsymbol{p}}_{ei}^2$, it follows from (28) that the right time derivative of $\bar{\boldsymbol{p}}_{ei}$ satisfies

$$D^+\bar{\boldsymbol{p}}_{ei} \leqslant \|\boldsymbol{\Delta}_i\| + \mu\sum_{j\in\bar{\mathcal{N}}_i} a_{ij}(\bar{\boldsymbol{p}}_{ej} - \bar{\boldsymbol{p}}_{ei}). \tag{29}$$

Denote $\bar{\boldsymbol{p}}_e = \mathrm{col}(\bar{\boldsymbol{p}}_{e1}, ..., \bar{\boldsymbol{p}}_{eN})$ and $\bar{\boldsymbol{\Delta}} = \mathrm{col}(\|\boldsymbol{\Delta}_1\|, ..., \|\boldsymbol{\Delta}_N\|)$. Then, N inequalities in the form of (29) can be written in the following compact form:

$$D^+\bar{\boldsymbol{p}}_e \leqslant -\mu H\bar{\boldsymbol{p}}_e + \bar{\boldsymbol{\Delta}}. \tag{30}$$

It follows from (30) and Lemma 1 that

$$\bar{\boldsymbol{p}}_e(t) \leqslant e^{-\mu H(t-t_0)}\bar{\boldsymbol{p}}_e(t_0) + \int_{t_0}^{t} e^{-\mu H(t-\tau)}\bar{\boldsymbol{\Delta}}(\tau)d\tau.$$

Since $\hat{v}_i(t)$ converges to $v_0(t)$ exponentially and $\hat{\theta}_{ei}(t) \to$ converges to $\theta_{ei}(t)$ exponentially as $t \to \infty$, $\boldsymbol{\Delta}_i(t)$ converges to zero exponentially as $t \to \infty$, i.e., there exist α_2, $\beta_2 > 0$ such that $\|\bar{\boldsymbol{\Delta}}\| \leqslant \alpha_2 e^{-\beta_2(t-t_0)}\|\bar{\boldsymbol{\Delta}}(t_0)\|$, $\forall t_0 \geqslant 0$.

Then, by (19), we have

$$\begin{aligned}\|\bar{\boldsymbol{p}}_e(t)\| &\leqslant \|e^{-\mu H(t-t_0)}\|\|\bar{\boldsymbol{p}}_e(t_0)\| + \int_{t_0}^{t}\|e^{-\mu H(t-\tau)}\|\|\bar{\boldsymbol{\Delta}}(\tau)\|d\tau\\ &\leqslant \alpha_1\|\bar{\boldsymbol{p}}_e(t_0)\|e^{-\beta_1(t-t_0)} + \int_{t_0}^{t}\alpha_1\alpha_2 e^{-\beta_1(t-\tau)-\beta_2(\tau-t_0)}\|\bar{\boldsymbol{\Delta}}(t_0)\|d\tau\\ &\leqslant \alpha_1\|\bar{\boldsymbol{p}}_e(t_0)\|e^{-\beta_1(t-t_0)} + \alpha_1\alpha_2\|\bar{\boldsymbol{\Delta}}(t_0)\|e^{\beta_2 t_0-\beta_1 t}\int_{t_0}^{t} e^{(\beta_1-\beta_2)\tau}d\tau.\end{aligned}$$

It follows that if $\beta_1 = \beta_2$,

$$\|\bar{\boldsymbol{p}}(t)\| \leqslant \alpha_1\|\bar{\boldsymbol{p}}(t_0)\|e^{-\beta_1(t-t_0)} + \alpha_1\alpha_2\|\bar{\boldsymbol{\Delta}}(t_0)\|e^{-\beta_1(t-t_0)},$$

otherwise it follows that

$$\|\bar{\boldsymbol{p}}(t)\| \leqslant \alpha_1\|\bar{\boldsymbol{p}}(t_0)\|e^{-\beta_1(t-t_0)} + \frac{\alpha_1\alpha_2}{\beta_1-\beta_2}\|\bar{\boldsymbol{\Delta}}(t_0)\|(e^{-\beta_1(t-t_0)} - e^{-\beta_2(t-t_0)}).$$

Thus, $\bar{\boldsymbol{p}}_e(t)$, i.e., each $\|\tilde{\boldsymbol{p}}_{ei}t)\|$, converges to zero exponentially as $t \to \infty$. This completes the proof. ∎

Now, we are ready to present the main result of Case 1.

Theorem 1. Problem 1 is solved by dynamic control law (11)–(15) under Assumptions 1–4, while velocity constraints (2) and (3) are satisfied. ∎

Proof. Define

$$\bar{v}_i = \mathrm{sat}(\hat{v}_i, \overline{v}, \underline{v}) - v_0, \tag{31}$$

and let

$$\boldsymbol{\chi}_i = [\boldsymbol{p}_{ei}\ \theta_{ei}]^{\mathrm{T}},\ \boldsymbol{\xi}_i = [\tilde{\boldsymbol{p}}_{ei}\ \tilde{\theta}_{ei}\ \bar{v}_i\ ]^{\mathrm{T}}. \tag{32}$$

The closed-loop system consisting of (10) and (11)–(15) can be written in the form of

$$\dot{\boldsymbol{\chi}}_i = \boldsymbol{f}(\boldsymbol{\chi}_i, v_0(t)) + \boldsymbol{g}(\boldsymbol{\chi}_i, \boldsymbol{\xi}_i, v_0(t)), \tag{33}$$

with

$$\boldsymbol{f}(\boldsymbol{\chi}_i, v_0(t)) = \begin{bmatrix}\omega_{ei}y_{ei} - v_{ei} + v_0\cos\theta_{ei}\\ -\omega_{ei}x_{ei} + v_0\sin\theta_{ei}\\ -\omega_{ei}\end{bmatrix},\ \boldsymbol{g}(\boldsymbol{\chi}_i, \boldsymbol{\xi}_i, v_0(t)) = \begin{bmatrix}y_{ei}(\omega_i-\omega_{ei}) - (v_i - v_{ei})\\ -x_{ei}(\omega_i-\omega_{ei})\\ -(\omega_i-\omega_{ei})\end{bmatrix}, \tag{34}$$

where

$$\omega_{ei} = \frac{k_2 v_0(y_{ei}\cos\frac{\theta_{ei}}{2} - x_{ei}\sin\frac{\theta_{ei}}{2}) + k_3\sin\frac{\theta_{ei}}{2}}{\sqrt{1+\boldsymbol{p}_{ei}^{\mathrm{T}}\boldsymbol{p}_{ei}}}, \tag{35}$$

$$v_{ei} = v_0 + \frac{k_1 x_{ei}}{\sqrt{1+\boldsymbol{p}_{ei}^{\mathrm{T}}\boldsymbol{p}_{ei}}}. \tag{36}$$

Then, Corollary 2.1 in [18] can be used to show that system (33) is uniformly stable at $\boldsymbol{\chi}_i = \mathbf{0}$ for all $\boldsymbol{\chi}_i \in \mathcal{X}$ with

$$\mathcal{X} = \{(x, y, \theta) | x \in \mathbb{R},\ y \in \mathbb{R},\ \theta \in (-2\pi,\ 2\pi)\}. \tag{37}$$

To show conditions (i)–(iii) in [18, Corollary 2.1] are satisfied, the remainder of the proof can be divided into the following three steps.

Step 1: Prove that the nominal system $\dot{\boldsymbol{\chi}}_i = \boldsymbol{f}(\boldsymbol{\chi}_i, v_0(t))$ is uniformly stable at $\boldsymbol{\chi}_i = \mathbf{0}$ for all $\boldsymbol{\chi}_i \in \mathcal{X}$.

Step 2: Show that $\boldsymbol{\xi}(t)$ converges to zero exponentially as $t \to 0$.

Step 3: Verify that $\boldsymbol{g}(\boldsymbol{\chi}_i, \boldsymbol{\xi}_i, v_0(t))$ satisfies

$$\|\boldsymbol{g}(\boldsymbol{\chi}_i, \boldsymbol{\xi}_i, v_0(t))\| \leqslant \|\boldsymbol{\xi}_i\| \Theta_1(\|\boldsymbol{\xi}_i\|) + \|\boldsymbol{\xi}_i\| \|\boldsymbol{\chi}_i\| \Theta_2(\|\boldsymbol{\xi}_i\|),$$

where $\Theta_1,\ \Theta_2 : \mathbb{R}_{\geqslant 0} \mapsto \mathbb{R}_{\geqslant 0}$ are continuous functions.

By Proposition 1, $\boldsymbol{\xi}(t)$ converges to zero exponentially as $t \to 0$, which completes the proof of Step 2. The proofs of Step 1 and Step 3 can be done by mimicking the proof of Theorem 3.1 in [18].

Finally, since v_0 and ω_0 satisfy Assumption 1 and $\frac{\tilde{x}_{ei}}{\sqrt{1+\hat{\boldsymbol{p}}_{ei}^{\mathrm{T}}\hat{\boldsymbol{p}}_{ei}}}$, $\frac{\tilde{y}_{ei}}{\sqrt{1+\hat{\boldsymbol{p}}_{ei}^{\mathrm{T}}\hat{\boldsymbol{p}}_{ei}}} \in (-1, 1)$, then k_1, k_2 and k_3 can be tuned by (16). Then, velocity constraints (2)–(3) can be satisfied. ∎

Remark 1. The design of the distributed observer (13)-(14) is different from that in [18] since a common reference direction is not available and $p_j - p_i$, θ_i, θ_j cannot be measured. The stability analysis for proving Proposition 1 can be established by using Lemma 1 which is not needed in the proof of Lemma 3.1 in [18]. ∎

3.2 Case 2: Limited Desired Relative Position

In this case, the assumption that $\omega_0(t) = 0$, $\forall t \geqslant t_0$, is not required, while the desired relative position $\boldsymbol{h}_{0i}$ needs to satisfy certain condition. In this case, the geometry of the formation cannot be arbitrarily set. Unlike Case 1, $\boldsymbol{h}_{0i}$ is assumed to be known to vehicle i. The assumption on Case 2 is summarized as follows.

Assumption 5. The desired relative position $\boldsymbol{h}_{0i}$ is a constant vector in the form of $\boldsymbol{h}_{0i} = [0\ r_i]^{\mathrm{T}}$, and is known to the follower vehicle i. ∎

First, define the tracking error $p_{ei} = [x_{ei}\ y_{ei}]^{\mathrm{T}}$ as

$$\boldsymbol{p}_{ei} = \boldsymbol{p}_0^i + \boldsymbol{h}_{0i},\ \theta_{ei} = \theta_0^i. \tag{38}$$

Taking its time derivative yields the following error dynamics:

$$\dot{\boldsymbol{p}}_{ei} = \omega_i S \boldsymbol{p}_{ei} + v_0 \begin{bmatrix} \cos\theta_{ei} \\ \sin\theta_{ei} \end{bmatrix} - v_i Q - \omega_i r_i Q,\ \dot{\theta}_{ei} = \omega_0 - \omega_i. \tag{39}$$

As in Case 1, we are aimed to show that $\boldsymbol{p}_e = \mathrm{col}(\boldsymbol{p}_{e1}, ..., \boldsymbol{p}_{eN})$ and $\boldsymbol{\theta}_e = \mathrm{col}(\theta_{e1}, ..., \theta_{eN})$ converge to zero as $t \to \infty$. Similar to that in Case 1, an internal state $[\hat{\boldsymbol{p}}_{ei}^{\mathrm{T}}\ \hat{\theta}_{ei}\ \hat{v}_i\ \hat{\omega}_i]^{\mathrm{T}}$ is set for each vehicle i. Let $\hat{\boldsymbol{p}}_{ei}$, $\hat{\theta}_{ei}$, $\hat{v}_i$, and $\hat{\omega}_i := \dot{\hat{\theta}}_{ei} + \omega_i$ be the estimate of $\boldsymbol{p}_{ei}$, θ_{ei}, v_0, and ω_0 for vehicle i respectively.

Then, we propose a dynamic control law for each follower vehicle i as follows.

$$v_i = \mathrm{sat}(\hat{v}_i, \overline{v}, \underline{v}) + \frac{k_{1i}\hat{x}_{ei}}{\sqrt{1 + \hat{\boldsymbol{p}}_{ei}^{\mathrm{T}}\hat{\boldsymbol{p}}_{ei}}} - w_i r_i, \tag{40}$$

$$\omega_i = \mathrm{sat}(\hat{\omega}_i, \overline{\omega}, -\overline{\omega}) + \frac{k_3 \sin\frac{\hat{\theta}_{ei}}{2}}{\sqrt{1 + \hat{\boldsymbol{p}}_{ei}^{\mathrm{T}}\hat{\boldsymbol{p}}_{ei}}} + \frac{k_2\, \mathrm{sat}(\hat{v}_i, \overline{v}, \underline{v})(\hat{y}_{ei}\cos\frac{\hat{\theta}_{ei}}{2} - \hat{x}_{ei}\sin\frac{\hat{\theta}_{ei}}{2})}{\sqrt{1 + \hat{\boldsymbol{p}}_{ei}^{\mathrm{T}}\hat{\boldsymbol{p}}_{ei}}}, \tag{41}$$

$$\begin{aligned} \dot{\hat{\boldsymbol{p}}}_{ei} = {} & \omega_i S \hat{\boldsymbol{p}}_{ei} + \hat{v}_i [\cos\hat{\theta}_{ei}\ \ \sin\hat{\theta}_{ei}]^{\mathrm{T}} - v_i Q - \omega_i r_i Q \\ & + \mu \sum_{j \in \mathcal{N}_i} a_{ij} (R(-\theta_j^i)\hat{\boldsymbol{p}}_{ej} - \hat{\boldsymbol{p}}_{ei} + \boldsymbol{p}_j^i + \boldsymbol{h}_{0i} - R(-\theta_j^i)\boldsymbol{h}_{0j}), \end{aligned} \tag{42}$$

$$\dot{\hat{\theta}}_{ei} = \frac{1}{\sum\limits_{j\in\mathcal{N}_i} a_{ij}} \sum_{j\in\mathcal{N}_i} a_{ij}((\hat{\omega}_j - \omega_i) + \mu(\hat{\theta}_{ej} - \hat{\theta}_{ei} + \theta_j^i)), \tag{43}$$

$$\dot{\hat{v}}_i = \frac{1}{\sum\limits_{j\in\mathcal{N}_i} a_{ij}} \sum_{j\in\mathcal{N}_i} a_{ij}(\dot{\hat{v}}_j + \mu(\hat{v}_j - \hat{v}_i)), \tag{44}$$

where μ is any positive constant, and k_{1i}, k_2, and k_3 are positive constants satisfying

$$k_{1i} \leqslant \min(v_{\max} - \overline{v} - \overline{\omega} r_i,\ \underline{v} - v_{\min} - \overline{\omega} r_i),\ 2k_2\overline{v} + k_3 \leqslant \omega_{\max} - \overline{\omega}. \tag{45}$$

The initial state $[\hat{\boldsymbol{p}}_{ei}^{\mathrm{T}}(t_0)\ \hat{\theta}_{ei}(t_0)\ \hat{v}_i(t_0)\ \hat{\omega}_i(t_0)]^{\mathrm{T}}$ can be arbitrarily selected in $\mathbb{R}^2 \times \mathbb{R} \times \mathbb{R} \times \mathbb{R}$. By default, $\hat{\boldsymbol{p}}_{e0} = [0\ 0]^{\mathrm{T}}$ and $[\hat{\theta}_{e0}\ \hat{v}_0\ \hat{\omega}_0]^{\mathrm{T}} = [0\ v_0\ \omega_0]^{\mathrm{T}}$. The implementation of dynamic control law (40)–(44) is similar to that in Case 1, and additionally requires vehicle j to send constant r_j and information $\hat{\omega}_i$ to vehicle i. The proposed control law also can be described in the form of (5).

To establish the main result of Case 2, a property of the distributed observer (42)–(44) is needed and is given in the following proposition.

Proposition 2. Consider the distributed observer (42)–(44), a leader vehicle and directed graph $\bar{\mathcal{G}}$. Under Assumptions 1–3 and 5, for any initial states $[\hat{\boldsymbol{p}}_{ei}^{\mathrm{T}}(t_0)\ \hat{\theta}_{ei}(t_0)\ \hat{v}_i(t_0)\ \hat{\omega}_i(t_0)]^{\mathrm{T}}$, $i = 1, ..., N$, $\forall t_0 \geqslant 0$, each $[\hat{\boldsymbol{p}}_{ei}^{\mathrm{T}}(t)\ \hat{\theta}_{ei}(t)\ \hat{v}_i(t)\ \hat{\omega}_i(t)]^{\mathrm{T}}$ converges to $[\boldsymbol{p}_{ei}^{\mathrm{T}}(t_0)\ \theta_0^i(t)\ v_0(t)\ \omega_0]^{\mathrm{T}}$ *exponentially* as $t \to \infty$. ∎

Proof. Define

$$\tilde{\boldsymbol{p}}_{ei} := [\tilde{x}_{ei}\ \tilde{y}_{ei}] = \hat{\boldsymbol{p}}_{ei} - \boldsymbol{p}_{ei},\ \tilde{\theta}_{ei} = \hat{\theta}_{ei} - \theta_{ei},\ \tilde{v}_i = \hat{v}_i - v_0,\ \tilde{\omega}_i = \hat{\omega}_i - \omega_0. \tag{46}$$

Using (43) and (46) yields

$$\sum_{j\in\mathcal{N}_i} a_{ij}(\dot{\tilde{\theta}}_{ej} - \dot{\tilde{\theta}}_{ei}) = -\mu \sum_{j\in\mathcal{N}_i} a_{ij}(\tilde{\theta}_{ej} - \tilde{\theta}_{ei}). \tag{47}$$

Defining $\delta_i = \sum_{j\in\mathcal{N}_i} a_{ij}(\tilde{\theta}_{ej} - \tilde{\theta}_{ei})$, (47) becomes

$$\dot{\delta}_i = -\mu\delta_i,\ i = 1, ..., N. \tag{48}$$

Then, denote $\tilde{\boldsymbol{\theta}}_e = \mathrm{col}(\tilde{\theta}_{e1}, ..., \tilde{\theta}_{eN})$, and we can obtain

$$[\delta_1, ..., \delta_N]^{\mathrm{T}} = \mu H \tilde{\boldsymbol{\theta}}_e. \tag{49}$$

It follows from (48) that $\delta_i(t) = e^{-(t-t_0)}\delta_i(t_0)$. Thus, $\tilde{\boldsymbol{\theta}}_e$ converges to zero exponentially as $t \to \infty$.

Denote $\hat{\boldsymbol{\omega}} = \mathrm{col}(\hat{\omega}_1, ..., \hat{\omega}_N)$. With $\hat{\omega}_0 = \omega_0$, we have

$$\left[\dot{\delta}_1, ..., \dot{\delta}_N\right]^{\mathrm{T}} = \mu H(\hat{\boldsymbol{\omega}} - \mathbf{1}_N \otimes \omega_0). \tag{50}$$

By (23), $\dot{\delta}_i(t)$ converges to zero exponentially as $t \to \infty$. Then, $\hat{\boldsymbol{\omega}}$ converges to $\mathbf{1}_N \otimes \omega_0(t)$ exponentially as $t \to \infty$. Similarly, we can prove that $\hat{v}_i(t)$ converges to $v_0(t)$ exponentially as $t \to \infty$.

Next, using (39), (42), (46), and $R(-\theta_j^i)\boldsymbol{p}_{ej} + \boldsymbol{p}_j^i + \boldsymbol{h}_{0i} - R(-\theta_j^i)\boldsymbol{h}_{0j} = \boldsymbol{p}_{ei}$ gives

$$\dot{\tilde{\boldsymbol{p}}}_{ei} = \omega_i S\tilde{\boldsymbol{p}}_{ei} + \mu \sum_{j\in\bar{\mathcal{N}}_i} a_{ij}(R(-\theta_j^i)\tilde{\boldsymbol{p}}_{ej} - \tilde{\boldsymbol{p}}_{ei}) + \boldsymbol{\Delta}_i, \tag{51}$$

which is the same as (26). The remainder of the proof can be referred to the proof of Proposition 1. ∎

Now, the main result of Case 2 is stated as follows.

Theorem 2. Problem 1 is solved by distributed dynamic control law (40)–(44) under Assumptions 1–3 and 5. Moreover, if

$$r_i < \min(\frac{v_{\max} - \overline{v}}{\overline{\omega}}, \frac{\underline{v} - v_{\min}}{\overline{\omega}}), \tag{52}$$

velocity constraints (2)–(3) are satisfied. ∎

Similar to Case 1, the proof of Theorem 2 can be done as follows.

Proof. Define

$$\bar{v}_i = \mathrm{sat}(\hat{v}_i, \overline{v}, \underline{v}) - v_0,\ \ \bar{\omega}_i = \mathrm{sat}(\hat{\omega}_i, \overline{\omega}, \underline{\omega}) - \omega_0, \tag{53}$$

and let

$$\boldsymbol{\chi}_i = [\boldsymbol{p}_{ei}\ \theta_{ei}]^{\mathrm{T}},\ \ \boldsymbol{\xi}_i = [\tilde{\boldsymbol{p}}_{ei}\ \tilde{\theta}_{ei}\ \bar{v}_i\ ]^{\mathrm{T}}. \tag{54}$$

The closed-loop system consisting of (10) and (11)–(15) can be written in the form of

$$\dot{\boldsymbol{\chi}}_i = \boldsymbol{f}(\boldsymbol{\chi}_i, \boldsymbol{\gamma}(t)) + \boldsymbol{g}(\boldsymbol{\chi}_i, \boldsymbol{\xi}_i, \boldsymbol{\gamma}(t)), \tag{55}$$

with $\boldsymbol{\gamma} := [v_0\ \omega_0]^{\mathrm{T}}$,

$$\boldsymbol{f}(\boldsymbol{\chi}_i, \boldsymbol{\gamma}(t)) = \begin{bmatrix} \omega_{ei} y_{ei} - v_{ei} + v_0 \cos\theta_{ei} \\ -\omega_{ei} x_{ei} + v_0 \sin\theta_{ei} \\ \omega_0 - \omega_{ei} \end{bmatrix},\ \ \boldsymbol{g}(\boldsymbol{\chi}_i, \boldsymbol{\xi}_i, \boldsymbol{\gamma}(t)) = \begin{bmatrix} y_{ei}(\omega_i - \omega_{ei}) - (v_i - v_{ei}) \\ -x_{ei}(\omega_i - \omega_{ei}) \\ -(\omega_i - \omega_{ei}) \end{bmatrix}, \tag{56}$$

where

$$\omega_{ei} = w_0 + \frac{k_2 v_0 (y_{ei} \cos\frac{\theta_{ei}}{2} - x_{ei} \sin\frac{\theta_{ei}}{2}) + k_3 \sin\frac{\theta_{ei}}{2}}{\sqrt{1 + \boldsymbol{p}_{ei}^{\mathrm{T}} \boldsymbol{p}_{ei}}}, \tag{57}$$

$$v_{ei} = v_0 + \frac{k_{1i} x_{ei}}{\sqrt{1 + \boldsymbol{p}_{ei}^{\mathrm{T}} \boldsymbol{p}_{ei}}} - \omega_{ei} r_i. \tag{58}$$

Then, the proof to show that system (55) is uniformly stable at $\boldsymbol{\chi}_i = \boldsymbol{0}$ for all $\boldsymbol{\chi}_i \in \mathcal{X}$ with $\mathcal{X} = \{(x, y, \theta) | x \in \mathbb{R},\ y \in \mathbb{R},\ \theta \in (-2\pi,\ 2\pi)\}$, is the same as that in the proof of Theorem 1.

Finally, noting that v_0 and ω_0 satisfy Assumption 1 and $\frac{\tilde{x}_{ei}}{\sqrt{1+\hat{\boldsymbol{p}}_{ei}^{\mathrm{T}}\hat{\boldsymbol{p}}_{ei}}}$, $\frac{\tilde{y}_{ei}}{\sqrt{1+\hat{\boldsymbol{p}}_{ei}^{\mathrm{T}}\hat{\boldsymbol{p}}_{ei}}} \in (-1, 1)$, if r_i satisfies (52), the parameters k_{1i}, k_2 and k_3 can be tuned based on (45) such that velocity constraints (2)–(3) are satisfied. ∎

Remark 2. The reason that Problem 1 is solved only in these two cases is given as follows. In a general case where $\boldsymbol{h}_{0i}$ is not limited and $\omega_0(t) = 0$, $\forall t \geqslant t_0$, is not satisfied, it is not possible to simultaneously make x_{ei}, y_{ei}, and θ_{ei} converges to zero. Mathematically, if $\omega_0(t) = 0$, $\forall t \geqslant t_0$, is not satisfied, the error dynamics in Case 1, i.e., (10) becomes

$$\dot{\boldsymbol{p}}_{ei} = \omega_i S \boldsymbol{p}_{ei} + v_0 \begin{bmatrix} \cos\theta_{ei} \\ \sin\theta_{ei} \end{bmatrix} - v_i Q - \omega_0 S R(-\theta_0^i) \boldsymbol{h}_{0i},\ \ \dot{\theta}_{ei} = -\omega_i. \tag{59}$$

Even if $[x_{ei}\ \theta_{ei}]^{\mathrm{T}}$ converges to zero, y_{ei} cannot converge to zero accordingly. This fact can be observed from the dynamics of y_{ei}, i.e.,

$$\dot{y}_{ei} = -\omega_i x_{ei} + v_0 \sin\theta_{ei} + \omega_0 [\cos\theta_{ei}\ \ \sin\theta_{ei}] \boldsymbol{h}_{0i}. \tag{60}$$

When $[x_{ei}\ \theta_{ei}]^{\mathrm{T}} = \boldsymbol{0}$, (60) becomes

$$\dot{y}_{ei} = \omega_0 [1\ \ 0] \boldsymbol{h}_{0i}. \tag{61}$$

There exists no control channel in the error dynamics (61), which results from the nonholonomic constraint $\dot{x}_i \sin\theta_i - \dot{y}_i \cos\theta_i = 0$ in each vehicle (1). It follows from (61) that $\dot{y}_{ei} = 0$ only if $[1\ \ 0]\boldsymbol{h}_{0i} = 0$, which coincides the assumption $\boldsymbol{h}_{0i} = [0\ r_i]^{\mathrm{T}}$ in Case 2.

Although ω_0 is not limited and the geometry of the formation is arbitrarily set in [18], yet it can be observed from (6) that the objective $\lim_{t\to\infty} \boldsymbol{p}_0^i(t) + \boldsymbol{h}_{0i} = 0$ is not as the same as that in [18]. Note that in [18], a common reference direction is required for all vehicles, and the result in [18] cannot applied to vehicles with local coordinate frames. ∎

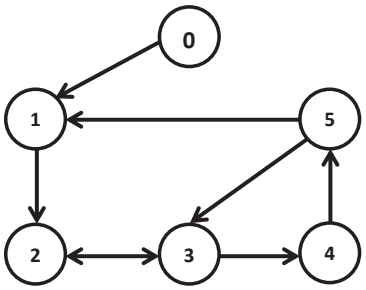

Fig. 2 The directed graph $\bar{\mathcal{G}}$ describing the network among vehicles.

Remark 3. In [15], formation of only one follower was studied, and the objective to make θ_{ei} converge to zero was not considered. While we take into account multiple followers and the objective $\lim_{t\to\infty}\theta_0^i(t)=0$. Besides, v_0 is allowed to be time-varying and the upper bound of v_i can be guaranteed. In [7], the network topology was assumed to be a directed acyclic graph and it was shown that the tracking error $\boldsymbol{p}_{ei}$ converges to a neighborhood of zero. While graph $\bar{\mathcal{G}}$ satisfying Assumption 3 includes graphs defined in [7] as a special case, and the proposed control law can make $\boldsymbol{p}_{ei}$ converge to zero in two cases. ■

Remark 4. The proposed control laws in this paper and those in [9, 10, 18] can be applied to the leader-following consensus problem of vehicles by setting $\boldsymbol{h}_{0i}$ to $\mathbf{0}$. Since a common reference direction is not required, the result in this paper has an advantage over those in [9, 10, 18] for solving the consensus problem. ■

Remark 5. In both cases, even though the follower vehicle can identify the leader, yet some followers cannot obtain the information of the leader, since the fixed network topology is prespecified and there exist no directed edges from the leader node to those follower nodes in $\bar{\mathcal{G}}$. Furthermore, in Case 1, each follower only knows $\boldsymbol{h}_{ji}$, $j\in\bar{\mathcal{N}}_i$ and has no knowledge of $\boldsymbol{h}_{0i}$. Thus, the problem in both cases cannot be simply divided into several tracking problems of a single vehicle. ■

4 Illustrative Examples

In this section, we verify effectiveness of the proposed control laws (11)–(15) and (40)–(44) in the described two cases respectively.

Consider 5 follower vehicles (labeled 1-5) which are desired to converge to the formation with respect to a leader vehicle (labeled 0). The directed graph $\bar{\mathcal{G}}$ is shown as in Fig. 2. The velocity constraints are given as $v_i\in[3-1.8\sqrt{2},\ 3+1.8\sqrt{2}]$ and $\omega_i\in[-0.671,\ 0.671]$. The bounds of the group reference velocities are $v_r^+=4.5$, $v_r^-=2$ and $\omega_r^+=0.3$. The initial states of follower vehicles, $[x_i(0)\ y_i(0)]^{\mathrm{T}}$ and $\theta_i(0)$, $i=1,..,N$, are listed in Table 1.

Table 1 The initial states of follower vehicles

Label	$[x_i(0)\ y_i(0)]^{\mathrm{T}}$	$\theta_i(0)$
1	$[-40\ 10]^{\mathrm{T}}$	π
2	$[-20\ -40]^{\mathrm{T}}$	$5\pi/6$
3	$[25\ -60]^{\mathrm{T}}$	0
4	$[50\ -0]^{\mathrm{T}}$	$-2\pi/3$
5	$[50\ 10]^{\mathrm{T}}$	0

In Case 1, the linear velocity and angular velocity of the leader vehicle are given as $v_0(t)=3.25-0.25\cos 0.24t$ and $\omega_0(t)=0$. Based on (16), tune the design parameters $k_1=1.5$, $k_2=0.0855$ and $k_3=0.5$. The initial state of leader is $[\boldsymbol{p}_0^{\mathrm{T}}\ \theta_0]^{\mathrm{T}}=[0\ 0\ \pi/6]^{\mathrm{T}}$. For follower vehicles, the desired relative positions to the leader are given by $[h_{01}^x\ h_{02}^x\ h_{03}^x\ h_{04}^x\ h_{05}^x]^{\mathrm{T}}=[-30\ -30\ 0\ 30\ 30]^{\mathrm{T}}$ and $[h_{01}^y\ h_{02}^y\ h_{03}^y\ h_{04}^y\ h_{05}^y]^{\mathrm{T}}=$

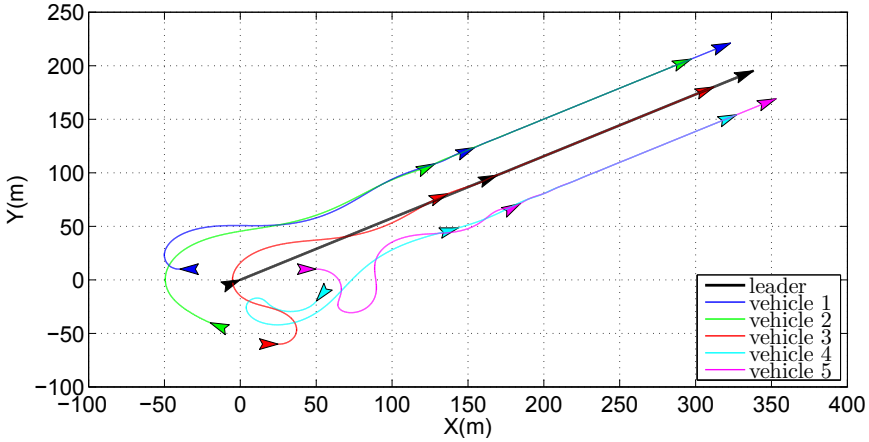

Fig. 3 Trajectories of all vehicles in Case 1.

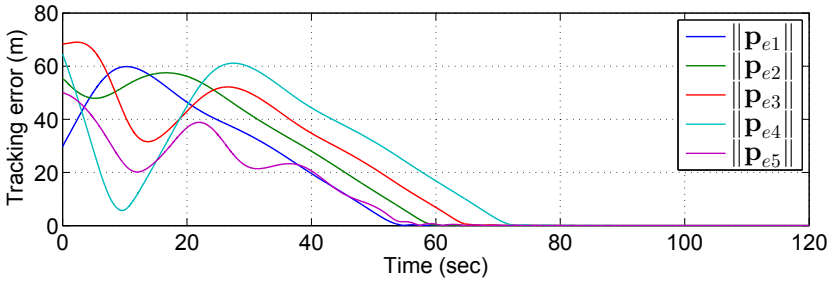

Fig. 4 Formation tracking errors $\|\boldsymbol{p}_{ei}\|(t)$ in Case 1.

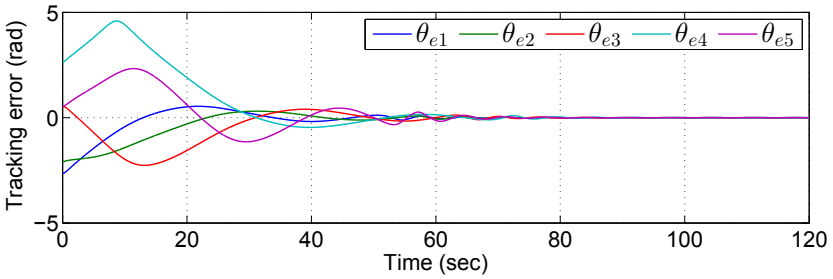

Fig. 5 Formation tracking errors $\theta_{ei}(t)$ in Case 1.

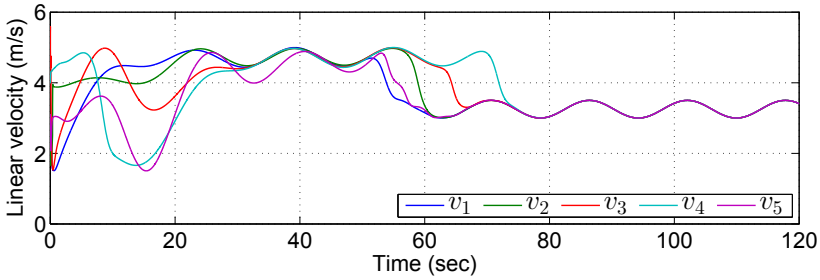

Fig. 6 Linear velocity of each vehicle $v_i(t)$ in Case 1.

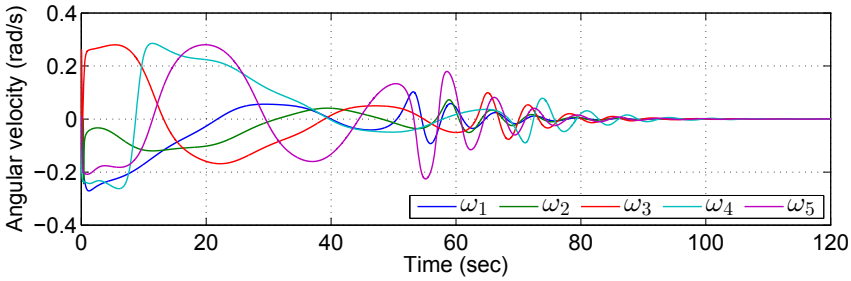

Fig. 7 Angular velocity of each vehicle $\omega_i(t)$ in Case 1.

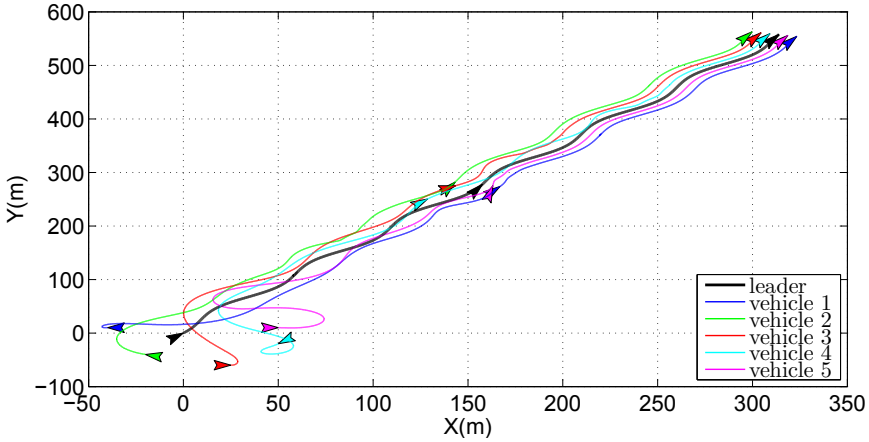

Fig. 8 Trajectories of all vehicles in Case 2.

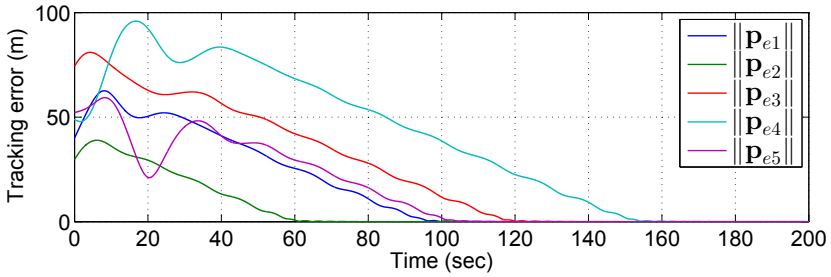

Fig. 9 Formation tracking errors $\|\boldsymbol{p}_{ei}\|(t)$ in Case 2.

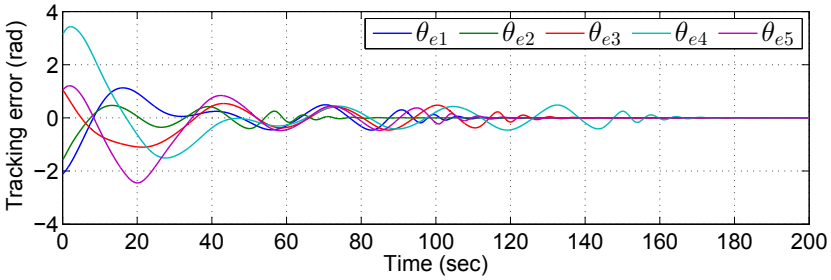

Fig. 10 Formation tracking errors $\theta_{ei}(t)$ in Case 2.

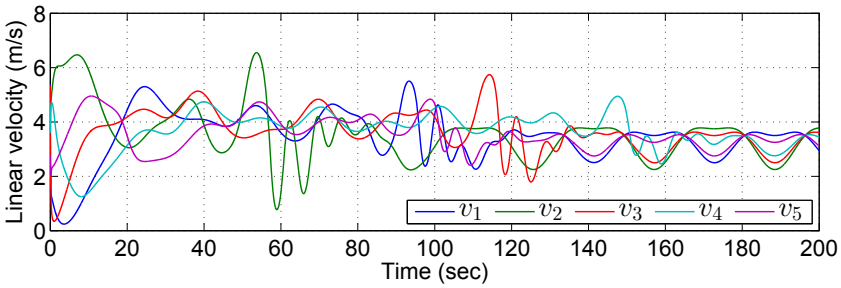

Fig. 11 Linear velocity of each vehicle $v_i(t)$ in Case 2.

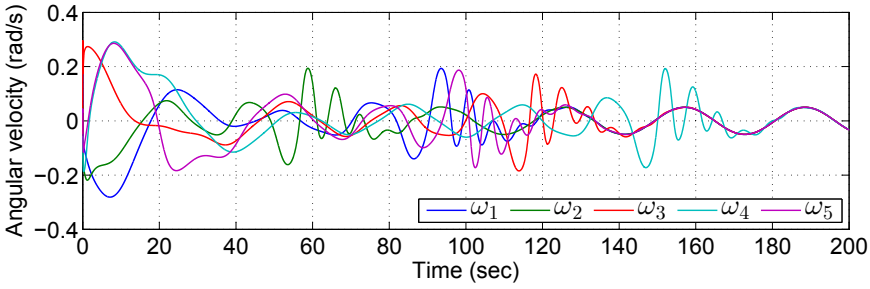

Fig. 12 Angular velocity of each vehicle $\omega_i(t)$ in Case 2.

$[0\ -30\ -30\ -30\ 0]^{\mathrm{T}}$. The initial states $[\hat{\boldsymbol{p}}_{ei}^{\mathrm{T}}(t_0)\ \hat{\theta}_{ei}(t_0)\ \hat{v}_i(t_0)]^{\mathrm{T}}$ of follower vehicles are listed in Table 2.

Table 2 The initial states of variables in (13)–(15)

Label	$\hat{\boldsymbol{p}}_{ei}^{\mathrm{T}}(0)$	$\hat{\theta}_{ei}(0)$	$\hat{v}_i(0)$
1	$[-15.51\ 22.86]^{\mathrm{T}}$	0.1π	3
2	$[-25.66\ -50.55]^{\mathrm{T}}$	0.7π	3.5
3	$[2.51\ -22.39]^{\mathrm{T}}$	-0.8π	4.5
4	$[79.72\ 12.81]^{\mathrm{T}}$	0.5π	2.5
5	$[20\ -18]^{\mathrm{T}}$	1.4π	2

Fig. 3 presents the trajectories of all vehicles during $0-120s$, which shows that the vehicles converge to the desired formation. Fig. 4 and Fig. 5 show that the formation tracking errors $\boldsymbol{p}_{ei}(t)$ and $\theta_{ei}(t)$ converge to zero respectively. Fig. 6 and Fig. 7 show that velocity constraints (2)–(3) are always satisfied.

In Case 2, the linear velocity and angular velocity of the leader vehicle are given as $v_0(t) = 1.25 - 0.25\cos 0.24t$ and $\omega_0(t) = 0.05\cos(0.2t)$. Based on (45), tune the design parameters $k_{1i} = 1.5$, $k_2 = 0.0855$ and $k_3 = 0.5$. The initial state of leader is $[\boldsymbol{p}_0^{\mathrm{T}}\ \theta_0]^{\mathrm{T}} = [0\ 0\ \pi/3]^{\mathrm{T}}$. For follower vehicles, the desired relative positions to the leader are given by $\boldsymbol{h}_{0i} = [0\ r_i]^{\mathrm{T}}$, $i = 1, ..., 5$, with $[r_1\ r_2\ r_3\ r_4\ r_5]^{\mathrm{T}} = [-10\ 15\ 10\ 5\ -5]$. The initial states $[\hat{\boldsymbol{p}}_{ei}^{\mathrm{T}}(t_0)\ \hat{\theta}_{ei}(t_0)\ \hat{v}_i(t_0)]^{\mathrm{T}}$ of follower vehicles are the same as listed in Table 2, and the initial states $\hat{\omega}_i(t_0)$ are $[\hat{\omega}_1(t_0)\ \hat{\omega}_2(t_0)\ \hat{\omega}_3(t_0)\ \hat{\omega}_4(t_0)\ \hat{\omega}_5(t_0)]^{\mathrm{T}} = [0.1\ -0.2\ 0.4\ 0.25\ -0.15]^{\mathrm{T}}$.

Fig. 8 presents the trajectories of all vehicles during $0-200s$, which shows that the vehicles converge to the desired formation. Fig. 9 and Fig. 10 show that the formation tracking errors $\boldsymbol{p}_{ei}(t)$ and $\theta_{ei}(t)$ converge to zero respectively. Fig. 11 and Fig. 12 show that velocity constraints (2)–(3) are always satisfied.

These simulation results illustrate effectiveness of the proposed control law.

5 Conclusion

In this paper, we have developed a distributed dynamic control law for networked unicycle-type vehicles, such that all follower vehicles with local coordinate frames converge to the desired leader-follower formation in two cases, while their velocity constraints including the constraint of positive-minimum linear velocity are always satisfied. For the future work, we will consider the internal uncertainties in the vehicle model and/or the external disturbances.

Appendix A Proof of Lemma 1

Lemma 1 is proved by the following two steps.

Proof. Step 1: Since $\boldsymbol{f}(t, \boldsymbol{y})$ is differentiable in t and locally Lipschitz in $\boldsymbol{y}$, then there exists a unique solution $\boldsymbol{y}(t)$ such that $\dot{\boldsymbol{y}} = \boldsymbol{f}(t, \boldsymbol{y})$, $\boldsymbol{y}(t_0) = \boldsymbol{y}_0$. For any $i = 1, 2, \cdots, n$, if $\boldsymbol{x} \leqslant \boldsymbol{y}$ and $x_i = y_i$ at time t, then it follows from the condition $\frac{\partial f_i(t,\boldsymbol{x})}{\partial x_j} \geqslant 0, \forall i \neq j$ that $f_i(t, \boldsymbol{x}) \leqslant f_i(t, \boldsymbol{y})$.

Step 2: Prove the lemma by contradiction. If there exist i_0 and $t_{i_0} \in [t_0, T)$ such that $x_{i_0}(t_{i_0}) > y_{i_0}(t_{i_0})$, then there must exist i, $t_1 \in [t_0, T)$ and $\delta > 0$ such that $x_i(t_1) = y_i(t_1)$, $x_i(t) > y_i(t)$ for $t \in (t_1, t_1 + \delta)$ and $\boldsymbol{x}_j(t_1) \leqslant \boldsymbol{y}_j(t_1)$ for any $j \neq i$. Then, $\boldsymbol{x}(t_1) \leqslant \boldsymbol{y}(t_1)$ holds. By Step 1, we have $f_i(t_1, \boldsymbol{x}(t_1)) \leqslant f_i(t_1, \boldsymbol{y}(t_1))$. Furthermore,

$$\begin{aligned} D^+x_i(t_1) &= \limsup_{\Delta t \to 0^+} \frac{x_i(t_1 + \Delta t) - x_i(t_1)}{\Delta t} \\ &> \limsup_{\Delta t \to 0^+} \frac{y_i(t_1 + \Delta t) - y_i(t_1)}{\Delta t} = \dot{y}_i(t_1). \end{aligned} \tag{A1}$$

However, it follows from (7) that $D^+x_i(t_1) \leqslant f_i(t_1, \boldsymbol{x}(t_1)) \leqslant f_i(t_1, \boldsymbol{y}(t_1)) = \dot{y}_i(t_1)$, which yields a contradiction.

The proof is thus completed. ∎

Acknowledgements This work was supported by the Research Grants Council of the Hong Kong Special Administrative Region of China under Project CityU/11213415.

Conflict of interest The authors declare that they have no conflict of interest.

References

1 Cao Y C, Yu W W, Ren W, Chen G R. An overview of recent progress in the study of distributed multi-agent coordination. IEEE Trans Ind Inf, 2013, 9(1): 427–438.

2 Chen J, Gan M G, Huang J, Dou L H, Fang H. Formation control of multiple euler-lagrange systems via null-space-based behavioral control. SCI CHINA Inf Sci, 2016, 59(1): 1–11.

3 Consolini L, Morbidi F, Prattichizzo D, Tosques M. Leader–follower formation control of nonholonomic mobile robots with input constraints. Automatica, 2008, 44(5): 1343–1349.

4 Gruszka A, Malisoff M, Mazenc F. Bounded tracking controllers and robustness analysis for UAVs. IEEE Trans Autom Control, 2013, 58(1): 180–187.

5 Huang P F, Wang D K, Meng Z J, Zhang F, Liu Z X. Impact dynamic modeling and adaptive target capturing control for tethered space robots with uncertainties. IEEE/ASME Trans Mechatron, 2016, 21(5): 2260-2271.

6 Kolmanovsky I and McClamroch N H . Developments in nonholonomic control problems. IEEE Control Syst, 1995, 15(6): 20–36.

7 Léchevin N, Rabbath C A, Sicard P. Trajectory tracking of leader–follower formations characterized by constant line-of-sight angles. Automatica, 2006, 42(12): 2131–2141.

8 Li X, Zhu D Q, Qian Y. A survey on formation control algorithms for multi-auv system. Unmanned Syst, 2014, 2(04): 351–359.

9 Liu T, Jiang Z P. Distributed formation control of nonholonomic mobile robots without global position measurements. Automatica, 2013, 49(2): 592–600.

10 Liu T, Jiang Z P. Distributed nonlinear control of mobile autonomous multi-agents. Automatica, 2014, 50(4): 1075–1086.

11 Oh K K, Park M C, Ahn H S. A survey of multi-agent formation control. Automatica, 2015, 53: 424–440.

12 Olfati-Saber R, Fax J A, Murray R M. Consensus and cooperation in networked multi-agent systems. Proc IEEE, 2007, 95(1): 215–233.

13 Qu Z. Cooperative control of dynamical systems: applications to autonomous vehicles. London: Springer-Verlag London Ltd, 2009.

14 Ren W, Beard R W. Trajectory tracking for unmanned air vehicles with velocity and heading rate constraints. IEEE Trans Control Syst, 2004, 12(5): 706–716.

15 Shen D B, Sun Z D, Sun W J. Leader-follower formation control without leader's velocity information. SCI CHINA Inf Sci, 2014, 57(9): 1–12.

16 Su Y F, Huang J. Cooperative output regulation of linear multi-agent systems. IEEE Trans Autom Control, 2012, 57(4): 1062–1066.

17 Wang N, Zhang T W, Xu J Q. Formation control for networked spacecraft in deep space: with or without communication delays and with switching topology. SCI CHINA Inf Sci, 2011, 54(3): 469–481.

18 Yu X, Liu L. Distributed formation control of nonholonomic vehicles subject to velocity constraints. IEEE Trans Ind Electron, 2016, 63(10): 1289–1298.

19 Zhang X Y, Duan H B, Yu Y X. Receding horizon control for multi-uavs close formation control based on differential evolution. SCI CHINA Inf Sci, 2010, 53(2): 223–235.